

Early Salient Region Selection Does Not Drive Rapid Visual Categorization

John K. Tsotsos, Iuliia Kotseruba, Calden Wloka
 York University, Toronto, Canada
 {tsotsos, yulia_k, calden @eecs.yorku.ca}

Abstract

The current dominant visual processing paradigm in both human and machine research is the feedforward, layered hierarchy of neural-like processing elements. Within this paradigm, visual saliency is seen by many to have a specific role, namely that of early selection. Early selection is thought to enable very fast visual performance by limiting processing to only the most relevant candidate portions of an image. Though this strategy has indeed led to improved processing time efficiency in machine algorithms, at least one set of critical tests of this idea has never been performed with respect to the role of early selection in human vision. How would the best of the current saliency models perform on the stimuli used by experimentalists who first provided evidence for this visual processing paradigm? Would the algorithms really provide correct candidate sub-images to enable fast categorization on those same images? Here, we report on a new series of tests of these questions whose results suggest that it is quite unlikely that such an early selection process has any role in human rapid visual categorization.

1. Introduction

The current dominant visual processing paradigm in both human and machine research is the learned, feedforward, layered hierarchical network of neural-like processing elements, with a history stretching from Rosenblatt's 1961 Perceptrons, Fukushima's 1975 Cognitron (and subsequent Neocognitron in 1982), to Rumelhart & McClelland's 1988 Parallel Distributed Processes, LeCun & Bengio's 1995 Convolutional Neural Networks, and to Krizhevsky, Sutskever, and Hinton's 2012 Deep Neural Networks. The goal of each of these models and systems was to explain or emulate the effortless ability of humans to immediately perceive content in images. Tsotsos (1988) termed this *immediate vision* and laid out the computational difficulty of the task as well as key elements of how brains and machines might defeat its combinatorial nature.

Our everyday experience tells us that vision feels immediate: we simply open our eyes and the world is there, fully formed before us and ready for our interactions. There is no perceptible time delay or inner 'turning of wheels'. It is well-documented over several decades that humans can recognize visual targets with remarkably short exposure times, with the seminal works including Potter & Levy (1969), Potter & Faulconer (1975), Potter (1975), Thorpe et al. (1996), and more recently Potter et al. (2014). The short exposure times (the shortest being 13ms) and subsequent fast responses (150ms of neural processing required for yes-no answers to categorize an image) led theoreticians to conclude that there was no time available for any processing other than a single pass through the visual hierarchy in the feedforward direction (e.g., Feldman & Ballard 1982)¹.

Still, the computational requirements to fully process a whole scene seem daunting (Tsotsos 1989) and many suggested that there must be some sort of optimizing action to reduce computational load occurring along that feedforward path. Within this paradigm, the processing of visual saliency has been suggested to have this specific role, namely reducing computational load via early selection (Koch & Ullman 1985). Early selection was thought to reduce the information that must be processed to enable very fast visual performance by determining a spatial region-of-interest (ROI) on which further analysis should be performed. In the Koch & Ullman formulation, a saliency map is computed early in the visual processing stream and represents point-wise stimulus conspicuity (contrast between a point and its local surround). A winner-take-all competition selects the most conspicuous location (point) and the features at the selected location are routed to a central representation for further processing. Inhibition of that selected location forces a shift to the next most conspicuous location when the algorithm is run again. Koch & Ullman's early selection idea seems to have been motivated by Feature Integration Theory (Treisman & Gelade 1980) in that it provided a mechanistic

¹ To be sure, there are a variety of models and theories that add feedback and recurrence to such hierarchical networks from Fukushima (1986) to Hochreiter & Schmidhuber (1997) and Sutskever (2012) and more, but with respect to the main thrust of this paper, these do not detract from the main conclusions here because they address tasks different from rapid visual categorization and thus, generally, would be inconsistent with the observed time course of human categorization performance.

version of its operation, specifically, the selection of a focus within the master map of locations. It shares much with the Early Selection model (Broadbent 1958), a model over which there has been substantial debate².

Early implementations of saliency computation did indeed produce points of maximum conspicuity that were found useful for machine vision (e.g., Clark & Ferrier (1988), Sandon (1990), Culhane & Tsotsos (1992), and Itti et al. (1998)). As algorithms evolved, they moved more towards salient region or object proposals (for reviews see Bylinskii et al. 2015, Bruce et al. 2015, Bylinskii et al. 2016). Fixation-based algorithms are typically validated by how well they match human fixation points (even though eye movements were not part of the original experimental work nor are they the only manifestation of attentional behaviour), while salient object detection algorithms are validated by how well the regions they produce overlap with ground truth object outlines or bounding boxes. The number of different saliency conceptualizations and implementations now is in the hundreds³. Models based on deep learning methods have also recently embraced this early selection idea in the hopes that their already impressive success can be improved further (e.g., Ba et al. 2014, Zhang et al. 2016).

Many high-profile models of human visual information processing, appearing over the past 3 decades, include some variant of early selection within a feedforward visual processing stream, including Sha’ashua & Ullman (1988), Olshausen et al. (1993), Itti & Koch (2001), Walther et al. (2002), Z. Li (2002, 2014), Deco & Rolls (2004), Itti (2005), Chikkerur et al. (2010), Zhang et al. (2011), Buschman & Kastner (2015) and more. These not only claim biological inspiration but also biological realism. That is, the authors claim that their processing strategies actually reflect the brain’s visual processing strategy. Often, it is difficult to evaluate such claims. The present work, however, examines one of the basic underlying features of all these models: that salience-based early selection within a feedforward visual hierarchy provides a spatial ROI on which further analysis is performed (i.e., the basic Koch & Ullman idea described above). Our motivation for this work was born from the observation that at least one set of critical tests of this idea has never been performed. No one has tested saliency models on the stimuli that were used in the seminal experiments that supported the feedforward view. Do these algorithms really provide an accurate reduction of the visual search space to enable fast categorization? Here, the first question we ask is: If the computation of saliency occurs early in the feedforward pass through visual areas, and determines a location for further processing, does the first ROI determined by a saliency algorithm effectively point to the target?

If the question were to be answered in the affirmative, then when the images used in the seminal experiments are run through a saliency algorithm, the algorithm should yield a prediction for the sub-image for further processing that matches well with the target location and extent. It would be reasonable to assume that if the sub-image is well predicted then categorization of its contents would be correct. That only the first selection of an algorithm is of interest is key: the temporal constraints provided by the experimental observations and which theorists used (e.g., Feldman & Ballard) do not permit more than one selection.

After conducting this experiment, the results pointed us to a second question: is human rapid visual categorization guided by early selection? This led to a second experiment, this time examining human behaviour, where we manipulated the stimulus image set to discover how much of a target is needed for good categorization. While addressing these two questions, we also examined other issues, specifically, center bias in datasets and algorithm biological plausibility. Together, the natural conclusion is that early selection played no role in the key seminal experiments. The remainder of the paper will detail these two experiments, but first the stimulus sets and performance measures used are described.

2. The Stimulus Datasets and Summary of Original Experimental Results

The following seminal experiments and image datasets were considered. Potter & Levy (1969) examined memory for visual events occurring at and near the rate of eye fixations. Their subjects were shown sequences of 16 pictures, from

² Broadbent suggested that in the first stage, ‘physical’ properties (focusing on audition, properties such as the pitch or location of sounds) would be extracted for all incoming stimuli, in a ‘parallel’ manner. In the second stage, more complex psychological properties, beyond simple physical characteristics (e.g. identity or meaning of spoken words), would be extracted. This second stage was more limited in capacity, so that it could not deal with all the incoming information at once when there were multiple stimuli (having to process them ‘serially’, rather than in parallel). A selective filter protected the second stage from overload, passing to it only those stimuli which had a particular physical property, from among those already extracted for all stimuli within the first stage. Many criticized Broadbent’s early selection idea and proposed alternates including late selection schemes Deutsch & Deutsch (1963), MacKay (1973), Moray (1969), Norman (1968), and attenuation schemes, Treisman (1964).

³ See the special issue of *Vision Research* on Computational Models of Visual Attention edited by Tsotsos, Eckstein and Landy (2016).

272 magazine photos, presented with rates of 0.5, 1, 2, 3, 4, 6, or 8 images per second. They concluded that rapidly presented pictures are processed separately for precisely the time each is in view and are not held with other items in a short-term memory. This was among the earliest works to demonstrate rapid categorization but the image set was unavailable for our use.

Potter and Faulconer (1975) used 96 stimuli, half of these being line drawings and half words that represent objects in those line drawings. There were 18 categories of objects and within each, between 2 and 9 instances (e.g., food: carrot, pie; clothing: hat, coat; tools: pliers, hammer). Each stimulus was preceded and followed by a mask of random lines and pieces of letters. Target information was provided to subjects in some trials before and, in others, after the stimulus. Stimuli were shown for 40, 50, 60 or 70ms. They observed that subjects needed 44ms exposure duration for the drawings and 46ms for the words to achieve 50% accuracy. We obtained these images and tested some of the saliency algorithms; however, we did not pursue these. The saliency algorithms all produced simply blurred versions of the line drawings and thus were not useful, likely due to their development being primarily based on natural images. This description is included here because it sets an early data point for fast categorization.

Potter (1975) used an RSVP (Rapid Serial Visual Presentation) task with 16 photos of natural scenes. Subjects were either shown the target that they might find within the sequence in advance or were told its name in advance. Accuracy was over 70% after only 125ms of exposure. In a second experiment, she tested subject's memory. Subjects looked at a 16-image sequence of pictures without prior instruction and were then asked a yes-no question about what they had seen. Subjects required about 300ms exposure to achieve 50% accuracy. Regrettably, this dataset was also unavailable.

Fortunately, there was an alternate stimulus set that was available. Potter et al. (2014) used an RSVP task of a series of six or 12 color pictures presented at 13, 27, 53 and 80ms per picture, with no inter-stimulus interval. Images were 300x200 in size, and there were 1711 images in total, 366 with target present. An example is shown in Figure 1a, with the corresponding hand-drawn ground truth mask (GTM). Participants were to detect a picture specified by a name (e.g., *smiling couple*) that was given just before or immediately after the sequence (in other words, subjects only had usable target expectations in half the trials). If subjects reported a positive detection, they were then asked a 2-alternative forced choice (2AFC) question to see if they could recognize the target given a distractor. Detection improved with increasing duration (from 13ms up to 80ms) and was generally better when the name was presented before the sequence, but performance was significantly above chance at all durations, whether the target was named before or after the sequence. At the shortest exposure, prior knowledge seemed to provide no benefit at all. For the set of trials without prior expectations, the ones relevant to our study, performance of the 2AFC task ranged from about 67% to about 73% correct on the target-present trials. Performance when prior expectation was provided ranged from 75-85% accuracy. The results are consistent with feedforward models, in which an initial wave of neural activity through the ventral stream is sufficient to allow identification of a complex visual stimulus in a single forward pass. Potter and her colleagues generously provided this dataset for our work and confirmed that these stimuli were of the same type as used in Potter & Levy (1969) and Potter (1975).

Thorpe et al. (1996) ran 'yes-no' categorization tasks. Subjects viewed color images that had been previously unseen, and had to determine if an animal was present or not (an example is shown in Figure 1b) The original images were 512x768 in size but downsized in Thorpe's experiment to 256x384 (which we used), with a total of 2000 images, with 996 having target present. An example is shown in Figure 1b. There was no prior knowledge of types of animals and stimuli were taken from commercial images. They measured behavior plus ERP (Event Related Potential). Even though the duration of the image exposure was 20ms, subjects exhibited 94% average correctness. Prefrontal ERP activity diverged at 150ms after stimuli onset for 'yes' and 'no' responses, which means enough processing has been done in 150ms to decide if an animal is present or not. They concluded that sufficient processing must be occurring in a primarily feedforward manner. Thorpe and colleagues graciously provided the full original dataset for our research⁴.

The two chosen experiments for our comparison are not identical and some justification as to why they are suitable for our test of feedforward saliency is in order. In the Thorpe et al. case, the processing path is direct and very much

⁴ Additional comments about this image set (Thorpe, personal communication, April 2, 2015): i. *adding extra groups of animals doesn't seem to make it harder for the visual system*; ii. *restricting the animal category to (say) birds, or dogs adds about 50ms to decision time. Basic level categories have no advantage*; iii. *the one animal that doesn't naturally fit are humans. Even though humans are of course animals, they appear to be in a different category completely*; and, iv. *statues of animals, and obvious pictures of animals (like pub signs with "The Horses Head") are not animals. But humans are very sophisticated at telling the difference. Indeed, when we were doing animal vs human faces, it was fascinating to see that even a child's face with makeup to look like a cat would never be treated as animal; we can spot the human beneath the makeup*.

what we need to compare against; if feedforward saliency computation is part of human categorization performance it would definitely be part of the 150ms time period Thorpe et al. reported. The most direct other experiment for us to include would have been the Potter (1975) paper. The closest we have to this is the Potter et al. (2014) stimulus set, confirmed to involve stimuli of the same type as the earlier paper. The detection component, which would reflect the same direct path as Thorpe et al., is present but was followed with an additional task. This means we should not compare time courses - and we do not. The detection task is reported using d' values, which are not the same as the measures we use and which do not permit us to recover % accuracy (positive hits). The 2AFC subsequent task, on the other hand, is reported using % accuracy, suitable for comparison. The 2AFC task was presented to subjects only for positive detection reports and asked if they saw a particular target with an onscreen question, with the stimulus no longer visible. If a saliency computation was present, then it would have played its role by that point and the 2AFC test yields a measure of short-term visual memory of the detection as a confirmation of the detection. We may thus assume that the positive hit rate of detection is at least as large as the accuracy of the 2AFC (but can say nothing about any error rates). Our comparison thus uses the largest reported 2AFC % accuracy in the following tests. We stress that our tests do not impact the validity of the original experiments.



Figure 1a. Sample images from the Potter dataset with target present (top left), no target present (top right), and corresponding ground truth masks (bottom row). In the experiment, participants were asked if they saw a particular target (here, "boys playing in the sand"). Only those trials where the question was asked after the stimulus presentation were used. The bottom panels show the hand-drawn ground truth masks; no-target images have no ground-truth.



Figure 1b. Sample images from the Thorpe dataset with target present (top left), no target present (top right), and corresponding ground truth masks (bottom row). In the experiment participants were asked if there is an animal in the image. The bottom panels show the hand-drawn ground truth masks; no-target images have no ground-truth.

3. Choices of Algorithms and Performance Measures

To conduct our test, we chose 7 bottom-up fixation based saliency models. Each is referred to by the acronym in bold given here. Two are algorithms that represent a cross-section of classical methods: the most commonly used and cited model by Itti et al. (1998) (**ITTI**) and the **AIM** model (Bruce & Tsotsos 2009), a consistently high performing model in benchmark fixation tests. We also selected several recent algorithms which achieved high scores in the MIT benchmark (Bylinskii et al. 2015b) and had publicly available source code, namely Saliency in Context (**SALICON**) by Huang et al. (2015), Boolean Map based Saliency (**BMS**) by Zhang & Sclaroff (2013), Ensembles of Deep Networks (**eDN**) by Vig et al. (2014), **RARE2012** by Riche et al. (2013), and **DeepGaze II** by Kümmerer et al. (2016). eDN, SALICON, and DeepGaze II represent the class of saliency algorithms based on deep learning. eDN model is a set of shallow neuromorphic networks selected via hyperparameter optimization for best performance on the MIT1003 saliency dataset (Judd et al. 2009). The other two models rely on transfer learning from deep networks initially trained on object classification tasks (VGG-19 in DeepGaze II and VGG-16 in SALICON) to achieve state-of-the-art performance on the MIT saliency benchmark. Finally, we also added the 'objectness' algorithm (**OBJ**)

because the human experiments all involve categorization of objects (Alexe et al. 2010)⁵. All algorithms were used with default parameters, with center bias disabled where applicable⁶, and published implementations (see Appendix A). A 9th method was added for control purposes, which we refer to as **CENTER**. This places the point of interest at the center of the image regardless of image contents. We use \mathcal{P} to denote the point of interest for all algorithms.

How one measures performance is very important especially when it involves direct comparison of human and machine output. In the absence of eye movements, the degree of overlap between a target and the region of high acuity in the retina is likely strongly correlated with human performance. As a result, some of our performance measures include this overlap. This seems easily justifiable by considering the details of human photoreceptor layout on the retina⁷. Observers in the original experiments were instructed to fixate the image center and there was no time for any change of gaze. Thus, if a sufficient spatial extent of the target lies within the observer's parafovea, it would seem that detection should be more likely correct.

If this assertion is appropriate, then image sets whose targets are strongly center-biased would lead to better categorization performance than those image sets with lesser bias. We thus created scatterplots for the target centroids of the two stimulus sets. This revealed a substantial center bias for the Potter set (Figure 2a) and a strong center bias for the Thorpe set (Figure 2b). Sure enough, Thorpe et al. reported higher human performance than Potter et al.

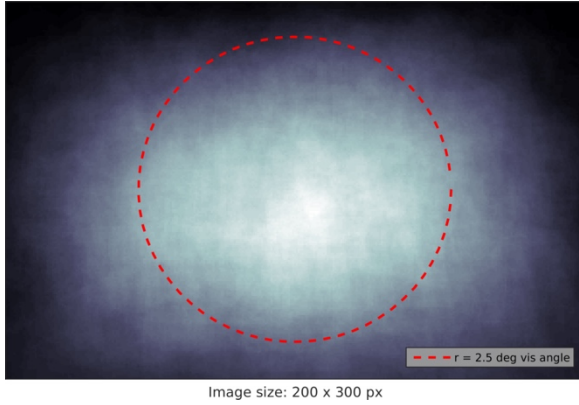


Figure 2a. A plot showing overlaid ground truth masks centroids for targets in the Potter dataset. Brighter pixels correspond to greater overlap between the masks. Parafovea ($r=2.5$ degrees of visual angle) is shown by a dashed red line. Mean of the distribution lies approximately in the center of the image. The area within 2.5 degrees of visual angle from the center of the image is calculated based on the following assumptions: the viewer is 57 cm away from the monitor, the monitor has 23" diagonal and resolution of 1920x1080.

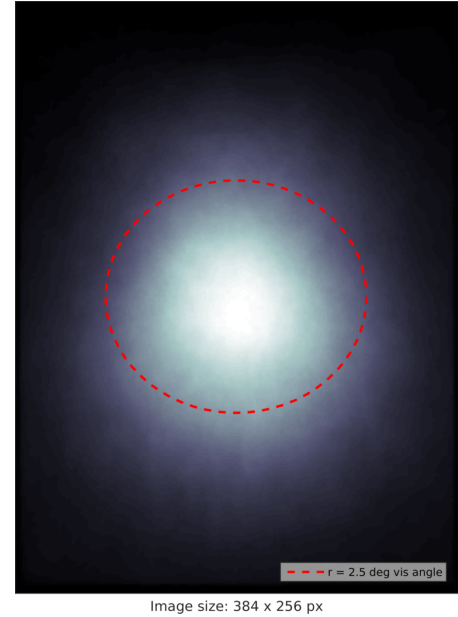


Figure 2b. A plot showing overlaid ground truth masks for targets in the Thorpe dataset. Brighter pixels correspond to greater overlap between the masks. Parafovea ($r=2.5$ degrees of vis angle) is shown by a dashed red line. Mean of the distribution lies approximately in the center of the image. The area within 2.5 degrees of visual angle from the center of the image is calculated based on the following assumptions: the viewer is 57 cm away from the monitor, the monitor has 23" diagonal and resolution of 1920x1080.

⁵ Normally OBJ outputs multiple object proposals as bounding boxes. These bounding boxes then can be combined to form a heatmap that approximately corresponds to a saliency map. The latter option was used in the experiments.

⁶ Many algorithms use an explicit center bias typically expressed as a centered Gaussian distribution in order to improve performance. These are detailed in Appendix A. This gain is rarely more than 2-3%. For those algorithms, this bias was disabled to enable a fair comparison.

⁷ Sources of relevant information on photoreceptor distribution and other retinal characteristics in humans include Østerberg (1935), Curcio et al. (1990), and Curcio & Allen (1990). Without recounting all the details, it is well-known that density of retinal cones is at its maximum at the very center of the fovea and falls rapidly towards the periphery. At its center lies the foveola, 350µm wide (0.5°) that is totally rod-free and capillary free, thus seeming the optimal target for new visual information. The parafovea is the region immediately outside the fovea with a diameter of 2.5mm (5°). It is important to recall that acuity decreases with retinal eccentricity. Anstis (1974) showed that to maintain visual acuity an object must increase by 2.76 arcmin in size for each degree of retinal eccentricity up to about 30°, and then somewhat more steeply up to 60°. It seems clear that if the target object that falls within the central 5° of the retina, the likelihood of its correct categorization is much higher than if otherwise.

How can a performance measure be defined that might reflect this? Thorpe et al. observed a 94% accuracy in their experiment; 94% of the targets had a least 27% of their extent within the parafovea. Similarly, Potter et al. observed accuracy of 73% and 73% of targets had at least 41% of their area within the parafovea. Samples of this calculation are shown in Figure 3⁸. Using these estimates, which are admittedly coarse at best, we limited the image region where a saliency algorithm prediction would be considered as a valid ROI cue for human categorization. Note that this is not a measure of algorithm correctness in the manner usually used in benchmark tests (e.g., Borji et al. 2015). The goal is to quantify how well saliency algorithms provide guidance for the human visual system towards the task of accurate image categorization. In any case, these are only two of the performance measures; the other two have no similar approximate nature.

We thus decided on four separate ways of quantifying algorithm performance. A saliency algorithm's predicted first point of interest, \mathcal{P} , would be marked as correct if:

- A) \mathcal{P} is anywhere within the GTM;
- B) \mathcal{P} is within the GTM AND within the parafovea, anywhere (even if by one pixel);
- C) \mathcal{P} falls within both the GTM AND the parafovea AND at least 27% of the GTM (by area) lies within the parafovea. This reflects the reality of Thorpe et al. data and will be applied only for those stimuli;
- D) \mathcal{P} falls within the GTM AND within the parafovea AND at least 41% of the GTM (by area) lies within the parafovea. This reflects the reality of Potter et al. data and will be applied only for those stimuli.

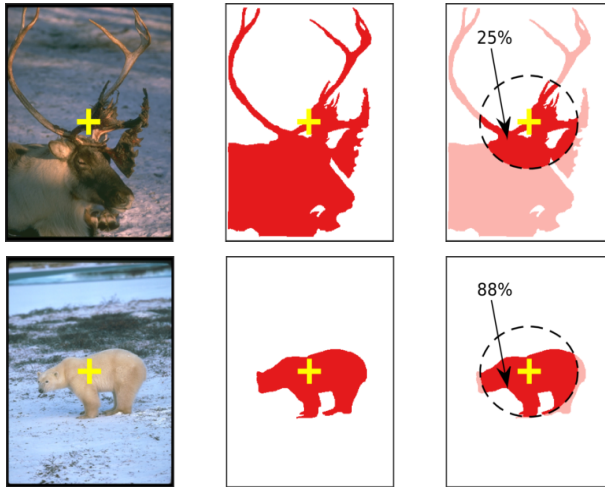


Figure 3. A visualization of the different quantitative performance measures we are using. Two examples are shown. The original stimulus image is on the left with the subject's fixation point marked. The middle image gives the ground truth mask where if the saliency algorithm produces a predicted \mathcal{P} , our measure A will count a positive hit. The right image shows the extent of the human parafovea, the dashed circle, centered at subject's fixation and superimposed on the GTM. Measure B will count a prediction as a hit if it falls within the marked area. Measure C and D will count a prediction as hit if measure B is a hit and the percentage of GTM area within the parafovea is sufficiently large. For these examples, 25% of the elk GTM area lies within the parafovea while the bear is 88% within. The elk image would lead to a 'hit' only for measures A and B whereas all the measures would count the bear as a hit.

When compared to the observed target layout characteristics, these are conditions which are very generous in favor of the algorithms. One additional point must be addressed. None of the tested algorithms include the capacity to accept prior instruction. The Potter et al. results we use as comparison are those without subjects receiving prior guidance while those of Thorpe included uniform guidance for expected category. Although this might appear to lead to an unfair comparison, we note that the performance in the Potter et al. (2014) experiment without prior expectation was roughly 10% lower than with prior guidance. As a result, we can reasonably assume a similar decrease in the Thorpe experiment, and as will be seen, this will not affect the overall conclusion.

4. Algorithm Performance

Figure 4 shows one example saliency heat map from each of the two datasets for each algorithm, one for a target-present and one for target-absent (the images used are those shown in Figure 1). The first problem with the categorization strategy of the early selection paradigm is revealed here, namely, that saliency produce a prediction for

⁸ To be sure, there is no correspondence between the set of observed correct responses, either per subject nor collectively, and the set of ground truth masks identified with this analysis. But such a correspondence cannot be computed with the available data and our purpose was not to correctly determine this correspondence. The purpose was to determine a guideline for how we measure algorithm correctness during our tests. An example of where this assumption may be inappropriate is the elk image of Figure 3.

all images irrespective of whether or not a target is present. That ROI is then passed along to the next stages for further processing. If it contains that target all is fine, but if it does not, the trial ends and it would remain unknown whether or not a target might be found anywhere else in the image. This is a fatal flaw for the whole approach unless a parallel method might be available that can make the correct global determination.

Figure 4a. (Left Panel) Saliency maps generated by 8 saliency algorithms for images from the Potter et al. dataset shown in Figure 1a with target present (left column) and no target present (right column). The red cross in each saliency map marks the global maximum found in the saliency map (the most likely first attended location predicted by the algorithm).

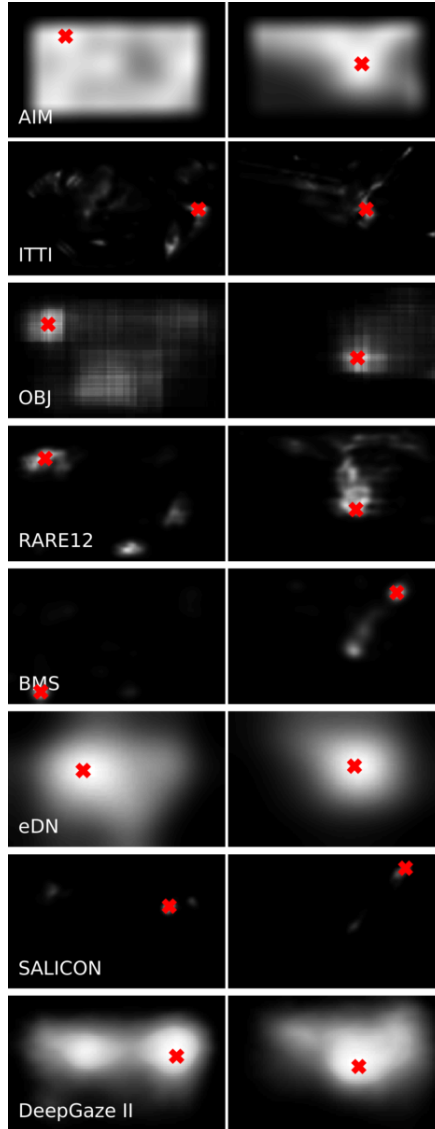
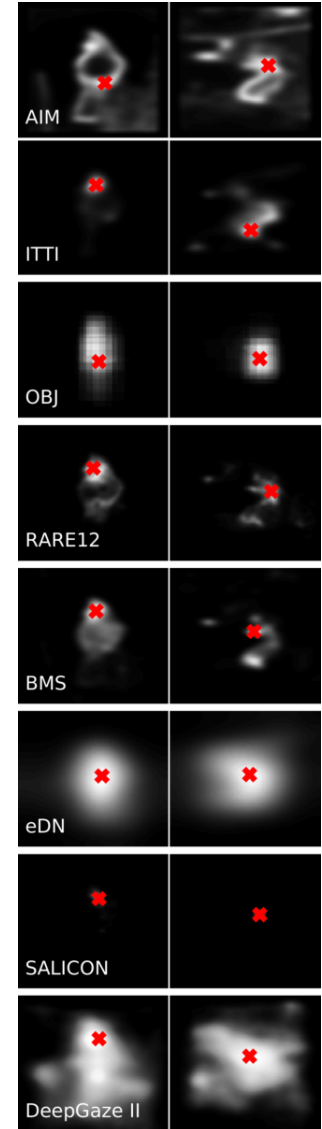


Figure 4b. (Right Panel) Saliency maps generated by 8 saliency algorithms for the images from the Thorpe et al. dataset shown in Figure 1b with target present (left column) and no target present (right column). The red cross in each saliency map marks the global maximum found in the saliency map (the most likely first location to attend predicted by the algorithm).



The overall categorization performance data is seen in Figure 5, where parts a, b, c and d correspond to the four performance measures described earlier, respectively.

This test reveals several results:

- Using the most generous measure, A, several algorithms approach human level performance.
- Using the more appropriate measure, B, only eDN approaches human performance on the Potter set and no algorithm comes close on the Thorpe dataset (even if reduced by 10% to compensate for instruction).
- Using the measure tailored for the Thorpe dataset, DeepGaze II is closest, but quite below human performance.
- Using the measure tailored for the Potter dataset, eDN leads the pack but again, somewhat below human performance.
- Interestingly, the CENTER algorithm works almost as well as the best algorithms and sometimes outperforms all methods.

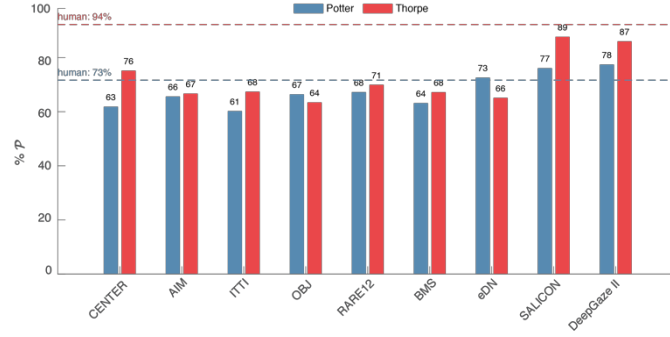


Figure 5a. Measure A - the percent of all first \mathcal{P} that fall anywhere within the GTM for each tested algorithm and dataset.

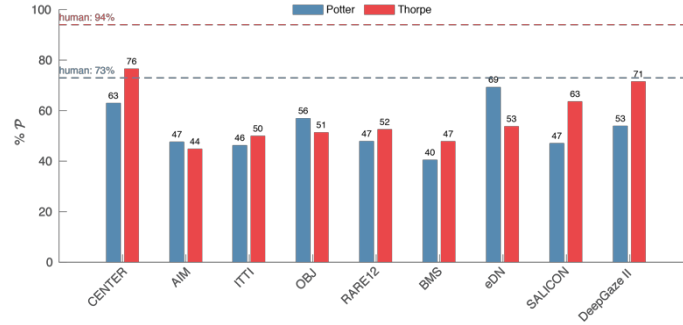


Figure 5b. Measure B - the percent of all first \mathcal{P} that fall that fall within the GTM AND within the parafovea for each tested algorithm and dataset.

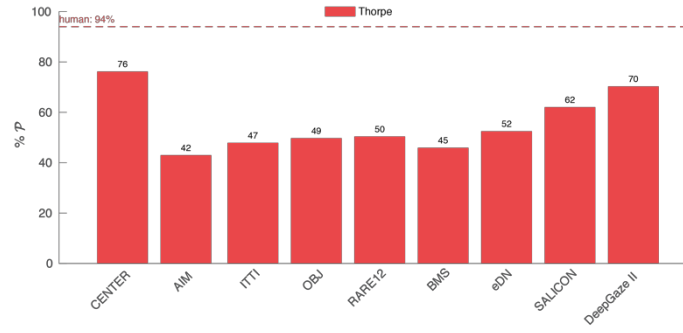


Figure 5c. Measure C - the percent of all first \mathcal{P} that fall within the GTM AND within the parafovea AND at least 27% of the GTM (by area) lies within the parafovea for each algorithm but for only the Thorpe images.

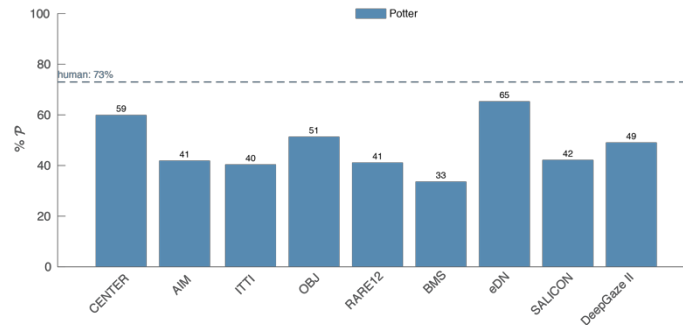


Figure 5d. Measure D - the percent of all first \mathcal{P} that fall within the GTM AND within the parafovea AND at least 41% of the GTM (by area) lies within the parafovea for each algorithm but only for the Potter images.

While performing these metric tests, we also plotted the locations of all the \mathcal{P} 's and these scatterplots are shown in Figure 6. It is easy to notice that there was a center bias in some cases as well as issues with boundary effects. Figure 6 shows scatterplots of algorithms' first \mathcal{P} location for the Potter dataset in parts *a* (target present) and *b* (target absent) and the same for the Thorpe dataset in parts *c* and *d*.

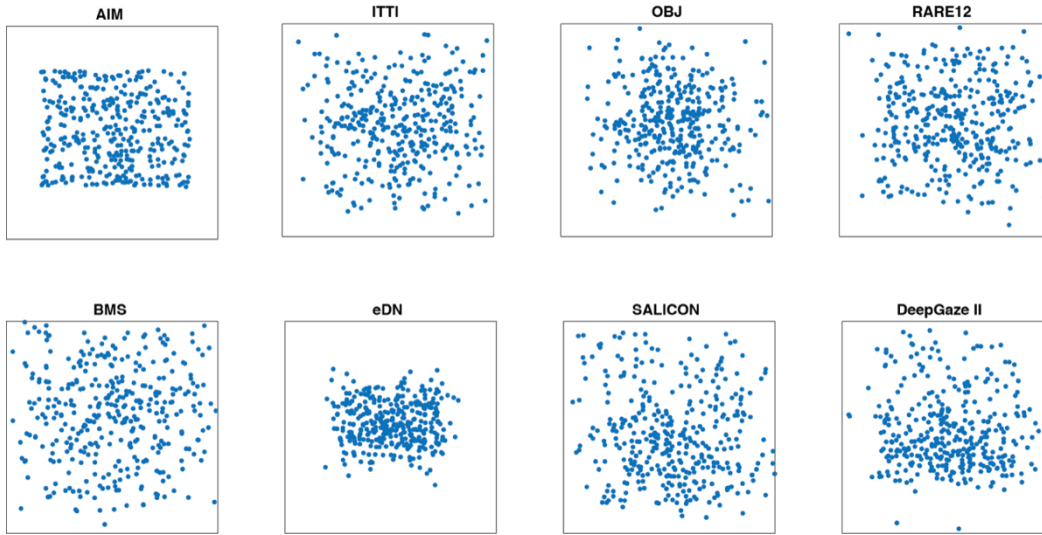


Figure 6a. Scatterplots showing the first attended locations predicted by the labeled saliency algorithm for the target-present images in the Potter set.

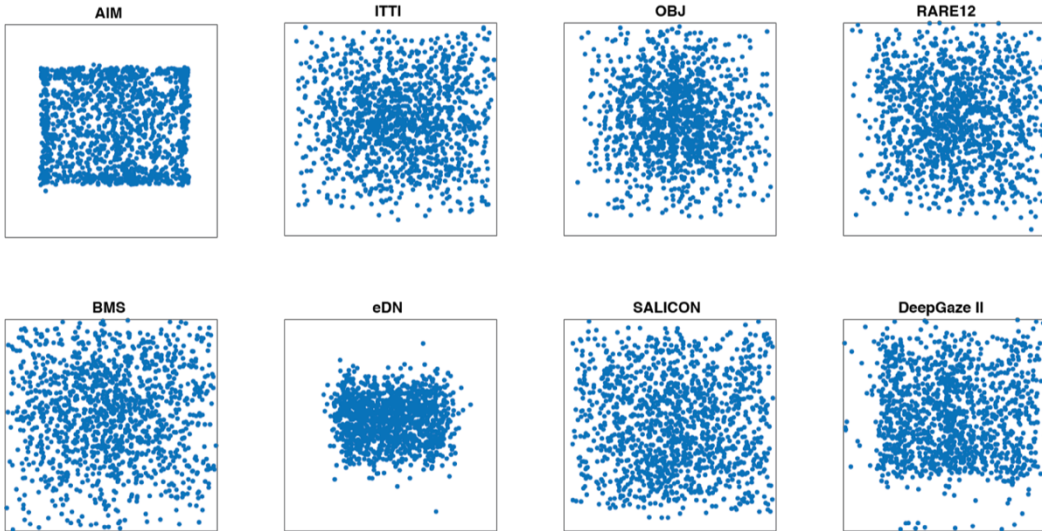


Figure 6b. Scatterplots showing first attended locations predicted by the labeled saliency algorithm for images with no target present from the Potter dataset.

The biases are striking. The AIM algorithm clearly has a problem with image boundaries⁹. ITTI, eDN, SALICON and DeepGaze II also seem to have a preference for more central \mathcal{P} results. It was shown earlier that the stimulus image sets do contain center bias for their targets; however, these algorithms demonstrate a center bias for the no-target cases as well. Even though we turned off explicit center bias computations for ITTI, eDN and DeepGaze II, it seems that these algorithms have additional center biases. Their good performance for the target-present cases is perhaps suspect as a result.

⁹ For AIM, this might be ameliorated through the use of image padding as the other algorithms employ, although this is not a biologically realistic solution.

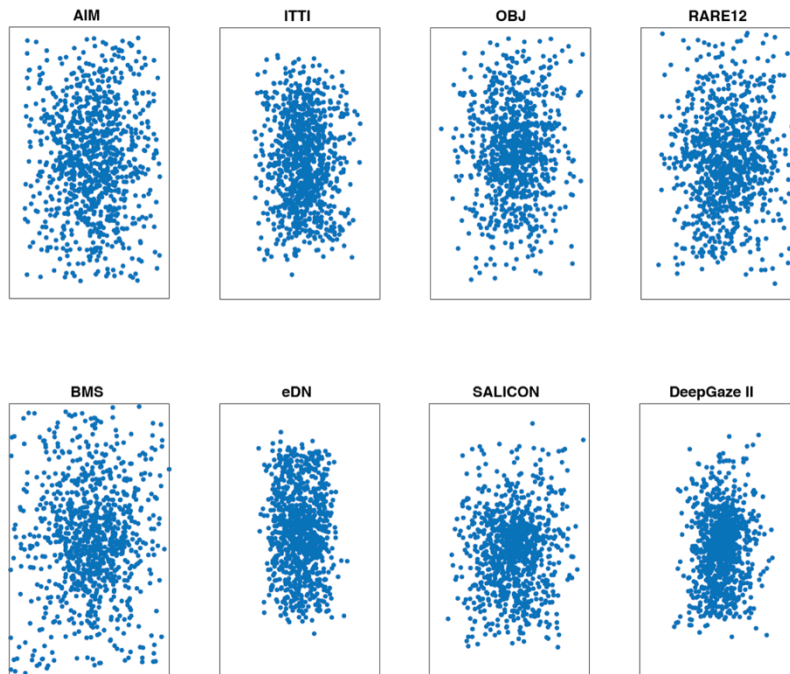


Figure 6c. Scatterplots showing the first attended locations predicted by the labeled saliency algorithm for the Thorpe target-present images.

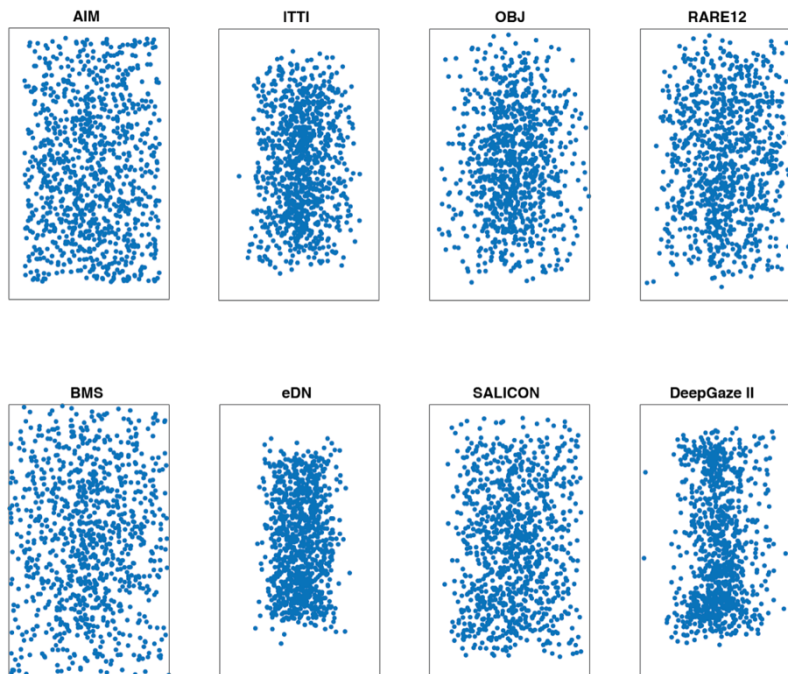


Figure 6d. Scatterplots showing first attended locations predicted by the labeled saliency algorithm for target-absent images absent from the Thorpe dataset.

5. Algorithm Biological Plausibility

Although many computer vision algorithms take significant inspiration from the human visual system, few embody that inspiration in a biologically realistic manner and most include extensions and enhancements in an attempt to outperform humans. It is difficult to evaluate such algorithms as to their biological plausibility but there is at least one tool that can be used. Feldman & Ballard (1982) explicitly linked computational complexity to neural processes saying "Contemporary computer science has sharpened our notions of what is 'computable' to include bounds on time, storage, and other resources. It does not seem unreasonable to require that computational models in cognitive science be at least plausible in their postulated resource requirements." They go on to examine the resources of time and numbers of processors, and more, leading to a key conclusion that complex behaviors can be carried out in fewer than one hundred (neural processing) time steps. These time steps were considered to be roughly the time it might take a single neuron to perform its basic computation (coarsely stated as a weighted sum of its inputs followed by a non-linear transformation) and then transmit its results to the next level of computation, perhaps about 10ms. Thorpe & Imbert (1989) also place similar constraints on processing time and numbers of layers suggesting that at least 10 layers of about 10msec per layer are needed. Combining this with Thorpe et al.'s observation that 150ms suffices for yes-no category decision, this constrains biologically plausible algorithms to those requiring no more than 15 or so layers of such computations. Since the algorithms we are testing do not deal with the full problem of categorization but only reflect the saliency computation stage, one might expect a much smaller time constraint, i.e., significantly fewer than 15 layers of computation.

Table 1 gives a coarse evaluation of the number of levels of computation, using the approximate criteria just described, for each of our tested algorithms. The AIM, BMS, ITTI, and eDN algorithms seem well within the timing constraints stated, with DeepGaze II and SALICON outside the constraint of significantly fewer than 15 layers. Of those that do fall within the time step constraint, only eDN shows good performance, primarily on the Potter set. The depth and style of computation of the DeepGaze II and SALICON algorithms mimics a full feedforward pass through the visual hierarchy. This perhaps argues for an incremental selection process which would be a valid possibility in human processing as well, although none of the models cited in this paper consider it (note Treisman's attenuated selection idea Treisman (1964)).

Algorithm	Processing Steps	Minimum Depth
AIM	Feature Filter → Density Estimation → Self-Information	3
BMS	Feature Split → Threshold Feature Channels → Connected Components + Normalization → Average + Dilation	4
ITTI	DoG and Gabor Filters → Average features + Normalization → Average channels + Normalization	3
eDN	Ensemble of CNNs (max. 3 layers) → SVM combination of CNN output	4
OBJ	4 Parallel Streams: [SR Saliency - depth 1; Patch colour contrast - depth 1; Edge detection → Edge counting - depth 2; Superpixel straddling - depth 5] → Bayesian integration	6*
RARE2012	PCA colour decomposition → log-Gabor filtering → Averaging and Normalization of log-Gabor scales → Gaussian pyramid + Density estimation → Self-information of channels → Weighted average within channels → Weighted average between channels	7
SALICON	VGG-16 fine-tuned to saliency detection	16
DeepGaze II	Extract features from VGG-19 → Readout network	19

Table 1. For each of the tested algorithms, an estimate of the number of neural-equivalent processing layers is presented. The AIM, BMS, ITTI, CAS, eDN algorithms seem within the timing constraints stated, with SALICON and DeepGaze II outside.

Notes: * The equivalent convolutional depth of the superpixel step is taken to be $\log(n)$ convolutions (where n is the number of pixels in the image), which works out to be approximately 5 layers for the images dealt with here.

6. Parafoveal Stimuli

The original stimulus set was revisited for human categorization performance to test the hypothesis that humans do not require the full image to achieve their high level of performance, and perhaps only the portion of the stimulus that is seen in an observer's parafovea was required. If the test images for rapid human categorization are center-biased as was demonstrated earlier for both the Thorpe and Potter datasets, this means there is little need for humans to require a shift in ROI if the subject's parafovea is at the image center since the target is usually right there too. This is

necessarily true since subjects are instructed to maintain a center gaze. One can thus ask whether the parafovea is a sufficient ROI so that there would be no need to adjust its position in order to obtain good performance.

We asked several questions:

- 1) What is the relationship between accuracy of categorization and the portion of the target that falls within the parafovea?
- 2) If the test images are cropped to be only the portion within the parafovea (that is, a circular region with 2.5° radius), what is human categorization performance?
- 3) What is the relationship between accuracy and portion of target within the parafovea for the 3 top performing algorithms (SALICON, eDN and DeepGaze II)?

The results are shown in Figures 7a, b, c respectively (the experimental procedure is detailed in Appendix B). The central red mark within each box indicates the median, and the bottom and top edges of the box indicate the 25th and 75th percentiles, respectively. The whiskers extend to the most extreme data points not considered outliers, and the outliers are plotted individually using the '+' symbol. Figure 7c shows performance of the top 3 saliency algorithms. Each algorithm was treated as an independent experimental subject. We used measure A to compute average accuracy on images within bins representing % of target covered by parafovea.

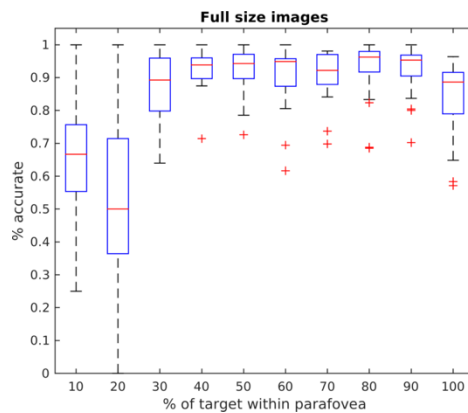


Figure 7a. A box plot showing human categorization performance, using the full, original images in Thorpe's dataset, plotted as a function of the percentage of the target within the parafovea. Recall that Thorpe reported 94% accuracy across the full image set.

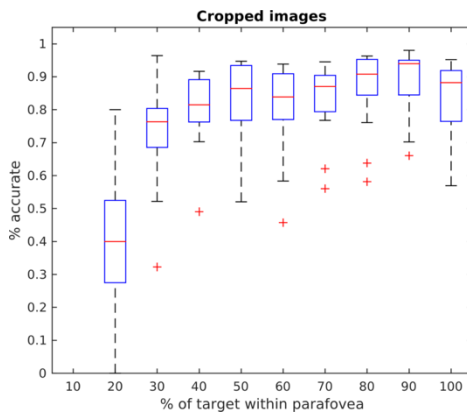


Figure 7b. A box plot showing human categorization performance, using images from Thorpe's dataset cropped so that the image portion outside the parafovea is set to a light grey, plotted as a function of the percentage of the target within the parafovea. Recall that Thorpe reported 94% accuracy across the full image set.

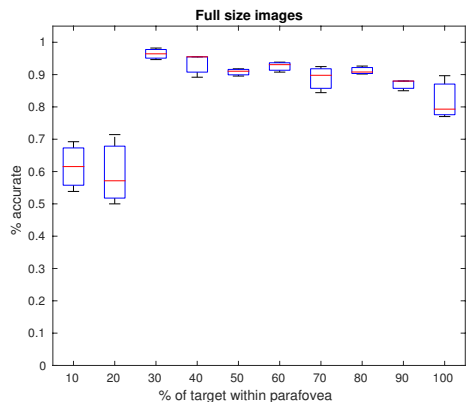


Figure 7c. A box plot showing performances of the top 3 saliency algorithms (SALICON, eDN and DeepGaze II). The plot shows the percentage of correct responses (vertical axis) vs the percentage of the target within the parafovea.

It appears that we were able to roughly duplicate Thorpe's results for the full, original images using his experimental parameters and protocol, as Figure 7a shows. High performance corresponded to at least 30% of the target being present in the parafoveal region. Even when the images are cropped to blank out extra-parafoveal portions, performance remained quite high as long as 30-40% of the target was inside the parafovea as seen in Figure 7b. Algorithm performance showed the same characteristic with the full images in Figure 7c; high accuracy was obtained whenever over 30% of the target was present in the parafovea. In other words, to a good approximation, both algorithm and human performance can be predicted by % target in the parafovea; setting a ROI within the image via any method would play little or no role. In addition, these results provide justification for our definition of performance Measures C and D given earlier; for the Thorpe images, we had defined a positive hit if \mathcal{P} falls within both the GTM AND the parafovea AND at least 27% of the GTM (by area) lies within the parafovea. From the results in Figure 7a, a figure perhaps closer to 30-35% might have been better. The definition we used was thus generous in favor of the algorithms.

7. Discussion

The analysis just presented is relevant only to the role saliency computation might play for human vision. It does not directly address the role of saliency in computer vision; however, it does highlight the fact that the use of saliency computation in computer vision might have no biological motivation or justification. There, it might well play an important role in limiting the extent of the image that needs to be processed by selecting more relevant image portions (there is a large literature on this already as mentioned above). We did, however, uncover some interesting, and not previously revealed, biases within several algorithms that certainly affect their overall performance:

- the AIM algorithm clearly has a problem with image boundaries;
- the ITTI, eDN, SALICON and DeepGaze II algorithms seem to have a preference for more central \mathcal{P} results (even after the built-in center bias was turned off for ITTI, eDN, DeepGaze II).

This places some doubt of on their strong performance for the target-present images.

The rest of this section will focus on several specific points of the analysis. The overall conclusion is that neither classic nor modern saliency algorithms, in their supporting role of ROI prediction, would lead to the same high level of categorization performance in humans. Further, a closer analysis of human performance shows that there is little point to an accurate feedforward point or region of interest prediction.

Firstly, it is important to explain why it is justified to test existing saliency algorithms in this manner when none of them can accept nor use task specifications or prior instruction. The only Potter results we use as comparison are those without subjects receiving prior guidance, while those we use of Thorpe included uniform guidance for expected category. Although this might appear to lead to an unfair comparison, we note that the performance in the Potter et al. (2014) experiment without prior expectation was roughly 10% lower than with prior guidance. As a result, we can reasonably assume a similar decrease in the Thorpe experiment. That is, accuracy would likely be only about 10% lower if subjects had no instruction as to category. van der Heijden et al. (1985) also reached a similar and thus consistent conclusion, finding a 12% relative change in performance between spatial cue present and absent conditions. If we reduce the Thorpe image set human performance by 10%, then in Figure 5a SALICON and DeepGaze II exceed human performance, but the conclusions from Figure 5b and 5c remain the same. Both algorithms do not seem to fit within the computational layer constraints. Finally, in Figure 7c, algorithm performance is shown comparable to human performance for sufficient target presence within the parafovea, i.e., the saliency prediction is not needed. Of course, the problem with no-target images remains.

There is a problem with the set of metrics we used that should be acknowledged. Following measures C or D for the elk image of Figure 3, none of the algorithms tested would give a correct hit if the predicted \mathcal{P} falls anywhere within the red region in the figure. This is not because of any fault of the algorithm but rather the definition of the metric itself which is tied to the position and scale of the target with respect to the observer's parafovea. This will lead to some amount of under-estimation of the accuracy of the algorithms, but the goal was to estimate how much of the target should be in the parafovea in order for a human to recognize it at the observed levels. It has already been acknowledged that the measure was not completely accurate. On the other hand, one can imagine an image where the target is small and completely within the parafovea, where a saliency algorithm hits it directly, but is not recognized by the observer because it is too small or may lie within distracting background elements. This would over-estimate accuracy with respect to humans. These two tendencies may balance each other to some degree. In addition, our human experiments, shown in Figure 7, inform us that the assumptions made in defining the measures C and D are reasonable.

It is certainly true that a better saliency algorithm that fits within the strategy first outlined by Koch & Ullman (1985) may yet be discovered. A still different possibility could be that even within the parafovea, some kind of early selection is taking place perhaps performing figure-ground segmentation and that selected figure is then passed on for further processing. But this seems to be simply changing the scale of the image; early selection within the fovea still has the same problem - how to be certain that a target is not elsewhere within the parafovea, and thus, this possibility does not suffice to solve the problem. With either possibility, the fact that the no-target images would remain incompletely processed remains.

It is a reasonable question to wonder what should the output of a saliency algorithm be for the no-target stimuli? Firstly, it seems important for the algorithm to include knowledge of what the target is. The classic saliency definition has no such component; it is purely a feedforward computation depending on local image contrast. Even if the definition changed to include such a top-down component, an output based on a maximal local contrast computation would not suffice. For a no-target stimulus, some separate, more global, computation seems required. Could it suffice to use a variance detector that gives a global measure of low variability across an image if there is no target? this is unlikely without knowledge of the target affecting the determination. In any case, this alone could not tell the difference between an image with only regions of low interest (i.e., low local contrast) and an image with many salient regions. It would seem that some absolute measure of saliency is needed rather than a relative one (something which is impossible to do when saliency maps normalize their output as standard practice). These characteristics no longer come close to the definition nor practice of saliency computations as seen between 1985 and the present. They may however, point to directions for future computational as well as human experimental work. This potential notwithstanding, the work reported here means that it is highly unlikely that a strictly feedforward and spatially local process - as the early selection concept dictates - can suffice to drive human rapid visual categorization.

8. Conclusions

The widely held position that visual saliency computation occurs early during the feedforward visual categorization process in human vision was tested and we found no support for it. It is emphasized that the conclusion applies only to human vision and not any saliency role useful for machine vision systems. In fact, our experiments have shown that many machine algorithms, freed from anatomical or resource constraints that bind the human visual system, perform very well.

This is not to say that saliency computation has no role in any other aspect of human vision. In Tsotsos et al. (2016) we describe a novel eye fixation prediction algorithm that employs several forms of saliency computation but not as selection for categorization tasks. It is a hybrid model that combines the positive elements of early selection, late selection, and more. We provide arguments that a cluster of conspicuity representations drives eye fixation selection, modulated by task goals and fixation history. Quantitative evaluation of this proposal shows performance that falls within the limits of human performance evaluation, and is far superior to any of the saliency methods tested (Wloka et al. 2018). Thus, visual saliency has at least the important role of participating in eye fixation computations.

Our experiments have shown that no tested algorithm can provide a sufficiently accurate first region-of-interest prediction to drive categorization results at human behaviour levels. In fact, little is gained by all the effort in comparison to the CENTER control model we tested. The many models and theories of human visual information processing, although inspiring and useful for many years of research, have served their role as important stepping stones on the path to understanding vision, but now may need to be reconsidered. Those saliency algorithms which do approach human performance seem too computationally expensive to also be biologically plausible as early selection mechanisms. It should be noted that the computational expense is not so large as to make them completely implausible; they could point to a continuous or incremental selection mechanism (as opposed to early or late) and this might be an interesting direction for future exploration. However, there is no provision in any algorithm for the target-absent stimuli. They cannot provide a 'no target' result in the same processing time; the salience-based processing strategy forces a serial search. We also tested human visual categorization and found that human performance seems to not need early salience. It appears sufficient for good categorization that some reasonable amount of the target appears in a subject's parafovea. Human performance was strongly predicted simply by the spatial relationship between target and the observer's parafovea, leading to the conclusion that a region-of-interest derived by any means adds little to human performance for conditions where gaze is fixed on the image center.

Acknowledgements

This research was supported by several sources, via grants to the senior author, for which the authors are grateful: Air Force Office of Scientific Research USA (FA9550-18-1-0054), Office of Naval Research USA (N00178-16-P-0087), the Canada Research Chairs Program (950-231659), and the Natural Sciences and Engineering Research Council of Canada (RGPIN-2016-05352). The human experimental portion of this paper was conducted under Certificate number 2016-014 (Selective tuning approach to visual system attention executive), Office of Research Ethics, York University. The authors are grateful for the datasets and advice provided by Simon Thorpe, Molly Potter, and Brad Wyble.

Appendix A

The code for all saliency algorithms is publicly available and was not modified for the experiments. Default parameters were used in each case. Below is a list of links.

AIM -	https://github.com/TsotsosLab/AIM
ITTI -	we use the implementation provided with the GBVS saliency package (http://www.vision.caltech.edu/~harel/share/gbvs.php)
OBJ -	v2.2 of the algorithm (http://groups.inf.ed.ac.uk/calvin/objectness/)
RARE2012 -	http://tcts.fpms.ac.be/attention/index.php?categorie1/models&model=001
BMS -	we use the most recent version for eye-fixation prediction presented in the 2015 PAMI paper (http://cs-people.bu.edu/jmzhang/BMS/BMS.html)
eDN -	https://github.com/coxlab/edn-cvpr2014
SALICON -	the original algorithm is not published; we use the open source version of it that has comparable results as described in the arXiv paper https://arxiv.org/abs/1606.00110 (https://github.com/CLT29/OpenSALICON)
DeepGaze II -	https://deepgaze.bethgelab.org/ (the code was not available at the time of the writing, so we used the saliency maps provided by the authors to our data)

In all experiments we used default parameters. In order to evaluate inherent center bias of the algorithms we turned off the explicit center prior used in the following saliency models: ITTI, eDN and DeepGaze II. Other algorithms in our selection do not use the explicit center prior.

Even though we switched off the explicit center prior where applicable, there is still a possibility that some models, in particular the deep learning ones, may learn center bias from the training data. For example, the OSIE dataset by Xu et al. (2014) (used to train the SALICON model), the SALICON dataset by Jiang et al. (2015) (used for the DeepGaze II model) and the MIT1003 dataset by Judd et al. (2009) (used for eDN) all have significant center bias.

Additional References

- Jiang, M., Huang, S., Duan, J., & Zhao, Q. (2015). Salicon: Saliency in context. In *Proceedings of the IEEE conference on computer vision and pattern recognition* (pp. 1072-1080).
- Judd, T., Durand, F., & Torralba, A. (2012). A benchmark of computational models of saliency to predict human fixations.
- Xu, J., Jiang, M., Wang, S., Kankanhalli, M. S., & Zhao, Q. (2014). Predicting human gaze beyond pixels. *Journal of vision*, 14(1), 28-28.

Appendix B

Experimental Details for the Parafoveal Stimuli Test of Section 6.0

Procedure

There are two conditions in the study. In the first condition, we replicate the experiment conducted by Thorpe et al. (1996). In the experiment subjects view an image for the duration of 20ms and perform a go/no-go categorization where they have to decide whether an animal is present in the scene or not. Since no specific task definition was provided in the original description of the experiment, we have asked our participants to look for a live animals excluding humans. In addition, the subjects were instructed to ignore artistic renditions of animals, such as those corresponding to drawings, statues, etc. In addition, see Footnote 4 above.

In the second condition, the images were cropped so that only the area within the circle with radius of 2.5 degrees of visual angle (corresponding to the size of the parafovea) remained visible. Subjects were instructed to maintain fixation on the cross presented and to not move their eyes. Each trial begins with a fixation cross for 500ms, followed by an image for 20ms and a fixation cross, on a blank screen, for 500ms. The images are shown consecutively with a random interval of 1 to 2 seconds during which subjects have to press the space bar on the keyboard if they see an animal in the image.

Participants

A total of 17 subjects (6 women, 11 men), between the age of 25 and 34 years old, participated in the study. All participants were volunteers and were not compensated for their participation. Additionally, the participants were asked to sign a consent form approved by the York University Office of Research Ethics. Each subject completed 10 blocks of 100 images for each condition.

Materials

The stimuli were 2000 color photographs as used in the original experiment in (Thorpe et al. 1996). The subjects were not familiar with the images and viewed each image only once. For each participant, the data was randomly split into two equally-sized sets for each experimental condition containing approximately the same number of images with and without animals. The images were resized to 256 by 384 pixels and were presented in the center of the monitor on a light gray background.

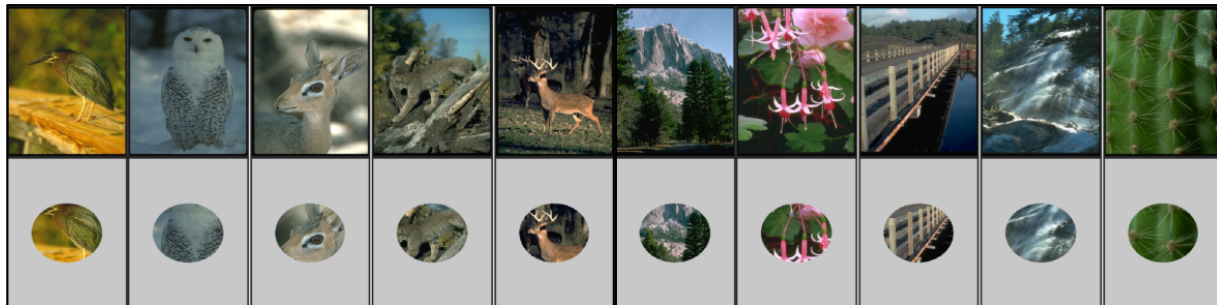


Figure B-1. Sample images from the Thorpe dataset with and without targets. The top row shows full images used in the first experimental condition and the bottom row shows the same images cropped to the size of the parafovea, used in the second experimental condition.

Apparatus

The experiments were programmed in Matlab R2016b using the Psychophysics Toolbox (Brainard 1997) version 3. The monitor, a ViewSonic Graphics Series GS815 19 in CRT, was set to 1024 x 768 resolution with 75 Hz refresh rate. All subjects were placed in a dark room and were seated 60 cm away from the monitor with their head movements restricted by a chin rest.

Results

The results of the first condition (full images) are similar to the ones reported by Thorpe et al. The average proportion of correct responses is 93% compared to the 94% in the original experiment. One of the subjects achieved the rate of 97% correct responses (98% in Thorpe et al.). In the second condition (cropped images) 85% of responses are correct

with a maximum of 91% achieved by one of subjects. In the second condition we excluded trials where the target was located outside the parafovea region (overall <1% of the trials were removed as a result). Examples of full-size and cropped images used in the experiment are shown in Figure B-1.

We analyzed individual participants' percentages of correct responses as a function of the percentage of overlap between the parafovea mask ($r=2.5^\circ$ visual angle) and a binary mask corresponding to the animal in the image. Only responses on target-present trials were considered for this analysis.

Figure B-1 show examples for the full-size (top row) and cropped images (bottom row) respectively. The results of the first experiment are shown in Figure 7a. Note that despite significant differences in individual performance, overall, most subjects have lower response accuracy when the target covers between 10 and 30% of the parafovea. The accuracy levels out when the target occupies >40% of the parafovea.

There is much more variability in the subject responses in the second experimental condition (cropped images), shown in Figure 7b, because most of the context is not available (see Figure B-1 bottom row). However, the same trend as in the first condition is still very noticeable. For instance, when the target occupies >20% of the parafovea, the average response accuracy is above 60%. Particularly, larger targets, covering >70% of the parafovea, were challenging because most of the animal was likely to be cropped out. Furthermore, in many cases, easily identifiable parts of the animals, such as head, wings, antlers, etc., are not necessarily present in the central region and for the images where the targets covered 100% of the parafovea, human/algorithm performance was a little worse.

We conducted a repeated-measures analysis of variance (ANOVA) on the human experimental data. The effect of target overlap with the parafovea on the accuracy of responses was significant in both conditions: $F(9, 144)=76.784 < 0.001$ and $F(9, 126)=100.305 < 0.001$ respectively.

Figure 7c shows the performance of the top 3 saliency algorithms (SALICON, eDN and DeepGaze II). Note that this plot is only provided for qualitative comparison since it was not possible to subject the algorithms to the same experimental conditions as human participants. For instance, response times are not comparable due the fact that humans are required to make motor responses. Furthermore, we generously assume that the target is recognized by the algorithm if the maximum of the saliency map falls within the ground truth mask (Measure A). Therefore, results shown in Figure 7c should be interpreted as the upper bound on the accuracy of the saliency algorithms.

Several observations can be made based on the box plots shown in Figure 7. First, the variance of the responses for the saliency algorithms (Figure 7c) is much lower than that of the human subjects (Figure 7b). Since the saliency algorithms are trained on human data, they highlight similar features in the images, particularly faces of humans and animals. Second, the percentage of correct responses monotonically improves as the target size, with respect to the parafovea, increases. Essentially, the larger the target, the higher are the chances that saliency maxima will fall within the ground truth mask.

References

- Alexe, B., Deselaers, T., Ferrari, V. (2010). What is an object? In *Proceedings of IEEE Conference on Computer Vision and Pattern Recognition*, pp. 73-80.
- Anstis, S. M. (1974). A chart demonstrating variations in acuity with retinal position. *Vision Research* 14, 589–592.
- Ba, J., Mnih, V., Kavukcuoglu, K. (2014). Multiple object recognition with visual attention. *arXiv preprint arXiv:1412.7755*.
- Borji, A., Cheng, M. M., Jiang, H., Li, J. (2015). Salient object detection: A benchmark. *IEEE Transactions on Image Processing*, 24(12), 5706-5722.
- Broadbent, D. (1958). **Perception and communication**, Pergamon Press, NY.
- Bruce, N.D., Wloka, C., Frosst, N., Rahman, S., Tsotsos, J.K. (2015). On computational modeling of visual saliency: Examining what's right, and what's left. *Vision Research* 116, 95-112.
- Bruce, N.D., Tsotsos, J.K. (2009). Saliency, attention, and visual search: An information theoretic approach. *Journal of Vision*, 9(3):5, 1-24.
- Buschman, T., Kastner, S. (2015). From Behavior to Neural Dynamics: An Integrated Theory of Attention, *Neuron* 88, p127-144.
- Bylinskii, Z., DeGennaro, E.M., Rajalingham, R., Ruda, H., Zhang, J., Tsotsos, J.K. (2015). Towards the quantitative evaluation of visual attention models. *Vision Research*, 116, 258-268.
- Bylinskii, Z., Judd, T., Borji, A., Itti, L., Durand, F., Oliva, A., Torralba, A. (2015b). MIT saliency benchmark.
- Bylinskii, Z., Judd, T., Oliva, A., Torralba, A., & Durand, F. (2016). What do different evaluation metrics tell us about saliency models? *arXiv preprint arXiv:1604.03605*.
- Chikkerur, S., Serre, T., Tan, C., Poggio, T. (2010). What and where: A Bayesian inference theory of attention. *Vision Research*, 50(22), 2233-2247.
- Clark, J.J., Ferrier, N. (1988). Modal Control of an Attentive Vision System. In *Proceedings of the IEEE International Conference on Computer Vision*, pp. 514-523.
- Clark, P.J., Evans, F.C. (1954). Distance to nearest neighbor as a measure of spatial relationships in populations. *Ecology* 35.4: 445-453.
- Cornia, M., Baraldi, L., Serra, G., Cucchiara, R. (2016). Predicting human eye fixations via an LSTM-based saliency attentive model. *arXiv preprint arXiv:1611.09571*.
- Curcio, C., Allen, K. (1990). Topography of ganglion cells in human retina, *Journal of Comparative Neurology*, 300, 5– 25.
- Curcio, C.A., Sloan, K.R., Kalina, R.E., Hendrickson, A.E. (1990). Human photoreceptor topography, *Journal of Comparative Neurology*, 292, 497 – 523.
- Culhane, S., Tsotsos, J. K. (1992). An Attentional Prototype for Early Vision. In *Proceedings of the European Conference on Computer Vision*, pp. 551-560.
- Deco, G., Rolls, E. T. (2004). A neurodynamical cortical model of visual attention and invariant object recognition. *Vision Research*, 44(6), 621-642.
- Deutsch, J., Deutsch, D. (1963). Attention: Some theoretical considerations. *Psychological Review*, 70, 80 – 90.
- Feldman, J., Ballard, D. (1982). Connectionist models and their properties. *Cognitive Science* 6, 205 – 254.
- Fukushima, K. (1975). Cognitron: A self-organizing multilayered neural network. *Biological cybernetics*, 20(3-4), 121-136.
- Fukushima, K., Miyake, S. (1982). Neocognitron: A self-organizing neural network model for a mechanism of visual pattern recognition. In *Competition and cooperation in neural nets* (pp. 267-285). Springer, Berlin, Heidelberg.
- Fukushima, K. (1986). A neural network model for selective attention in visual pattern recognition, *Biological Cybernetics*, 55 (1), 5 – 15.
- Goferman, S., Zelnik-Manor, L., Tal, A. (2012). Context-Aware Saliency Detection. *IEEE Transactions on Pattern Analysis and Machine Intelligence*, 34:1915-1926.
- Hochreiter, S., Schmidhuber, J. (1997). Long short-term memory. *Neural Computing* 9, 1735–1780.
- Huang, X., Shen, C., Boix, X., Zhao, Q. (2015). Salicon: Reducing the semantic gap in saliency prediction by adapting deep neural networks. In *Proceedings of IEEE International Conference on Computer Vision*, pp. 262-270.
- Itti, L., Koch, C., Niebur, E. (1998). A Model of Saliency-Based Visual Attention for Rapid Scene Analysis. *IEEE Transactions on Pattern Analysis and Machine Intelligence*, 20(11):1254-1259.
- Itti, L., & Koch, C. (2001). Computational modelling of visual attention. *Nature reviews neuroscience*, 2(3), 194.
- Itti, L. (2005). Models of bottom-up attention and saliency. In **Neurobiology of attention**, Eds. Itti, L., Rees, G., & Tsotsos, J., pp 576-582.
- Judd, T., Ehinger, K., Durand, F., Torralba, A. (2009). Learning to predict where humans look. *Int. Conference on Computer Vision*, p. 2106–2113.

- Koch, C., Ullman, S. (1985). Shifts in selective visual attention: Towards the underlying neural circuitry. *Human Neurobiology*, 4, 219 – 227.
- Kümmerer, M., Wallis, T. S., Bethge, M. (2016). DeepGaze II: Reading fixations from deep features trained on object recognition. *arXiv preprint arXiv:1610.01563*.
- Krizhevsky, A., Sutskever, I., & Hinton, G. E. (2012). ImageNet classification with deep convolutional neural networks. In *Advances in neural information processing systems* (pp. 1097-1105).
- LeCun, Y., Bengio, Y. (1995). Convolutional networks for images, speech, and time series. **The handbook of brain theory and neural networks**, Ed. Arbib M.A. MIT Press, pp. 255–258.
- Li, Z. (2002). A saliency map in primary visual cortex. *Trends in Cognitive Sciences*, 6 (1), 9 – 16.
- MacKay, D. (1973). Aspects of the theory of comprehension, memory and attention. *Quarterly Journal of Experimental Psychology*, 25, 22 – 40 .
- Moray, N. (1969). **Attention: Selective processes in vision and hearing**. London : Hutchinson .
- Norman, D. (1968). Toward a theory of memory and attention. *Psychological Review*, 75 , 522 – 536 .
- Olshausen, B. A., Anderson, C. H., Van Essen, D. C. (1993). A neurobiological model of visual attention and invariant pattern recognition based on dynamic routing of information. *The Journal of Neuroscience*, 13(11), 4700-4719.
- Østerberg, G.A. (1935). Topography of the layer of rods and cones in the human retina, *Acta Ophthalmologica* 6 Suppl, 1 – 102.
- Potter, M. C., Faulconer, B. A. (1975). Time to understand pictures and words. *Nature*, 253(5491), 437-438.
- Potter, M. C. (1975). Meaning in visual search. *Science*, 187(4180), 965-966.
- Potter, M.C., Levy, E.I. (1969). Recognition memory for a rapid sequence of pictures. *Journal of Experimental Psychology*, 81(1), 10-15.
- Potter, M. C., Wyble, B., Haggmann, C. E., McCourt, E. S. (2014). Detecting meaning in RSVP at 13ms per picture. *Attention, Perception, & Psychophysics*, 76(2), 270-279.
- Riche, N., Mancas, M., Duvinage, M., Mibulumukini, M., Gosselin, B., & Dutoit, T. (2013). RARE2012: A multi-scale rarity-based saliency detection with its comparative statistical analysis. *Signal Processing: Image Communication*, 28(6), 642–658.
- Rosenblatt, F. (1961). **Principles of neurodynamics: Perceptions and the theory of brain mechanisms**, Washington, DC, Spartan Books.
- Rumelhart, D. E., McClelland, J. L. (1986). **Parallel distributed processing: Explorations in the microstructure of cognition**, MIT Press
- Sandon, P. (1990). Simulating visual attention. *Journal of Cognitive Neuroscience*, 2(3), 213 – 231.
- Sha'ashua, A., Ullman, S. (1988). Structural saliency: The detection of globally salient structures using a locally connected network. In *Proceedings of International Conference on Computer Vision*, pp. 321-327.
- Sutskever, I. Training Recurrent Neural Networks. PhD thesis, University of Toronto (2012).
- Thorpe, S. J., & Imbert, M. (1989). Biological constraints on connectionist modelling. *Connectionism in perspective*, 63-92.
- Thorpe, S., Fize, D., Marlot, C. (1996). Speed of processing in the human visual system. *Nature*, 381(6582), 520-522.
- Treisman, A., Gelade, G. (1980). A feature integration theory of attention. *Cognitive Psychology*, 12, 97-136.
- Treisman, A. (1964). The effect of irrelevant material on the efficiency of selective listening, *American Journal of Psychology*, 77, 533 – 546.
- Tsotsos, J. K., Eckstein, M. P., Landy, M. S. (2015). Computational models of visual attention. *Vision Research*, 116(Pt B), 93.
- Tsotsos, J.K. (1988). A Complexity Level Analysis of Immediate Vision, *International Journal of Computer Vision*, Marr Prize Special Issue, 2(1), 303-320, Sept. 1988.
- Tsotsos, J.K. (1989). The Complexity of Perceptual Search Tasks. In *Proceedings of 11th International Joint Conference on Artificial Intelligence*, pp. 1571 – 1577.
- Tsotsos, J.K. (2011). **A Computational Perspective on Visual Attention**, MIT Press
- Tsotsos, J., Kotseruba, I., Wloka, C. (2016). A Focus on Selection for Fixation. *Journal of Eye Movement Research*, 9(5), p1-34.
- Vig, E., Dorr, M., Cox, D. (2014). Large-Scale Optimization of Hierarchical Features for Saliency Prediction in Natural Images. In *Proceedings of IEEE Conference on Computer Vision and Pattern Recognition*, pp. 2798–2805.
- van der Heijden, A. H., Schreuder, R., Wolters, G. (1985). Enhancing single-item recognition accuracy by cueing spatial locations in vision. *The Quarterly Journal of Experimental Psychology Section A*, 37(3), 427-434.
- Walther, D., Itti, L., Riesenhuber, M., Poggio, T., Koch, C. (2002). Attentional selection for object recognition—a gentle way. In *Biologically Motivated Computer Vision* (pp. 472-479). Springer Berlin Heidelberg.

- Wloka, C., Kotseruba, I, Tsotsos, J.K. (2018). Active Fixation Control to Predict Saccade Sequences. In *Proceedings of IEEE Conference on Computer Vision and Pattern Recognition*, pp. 3184-3193.
- Zhang, Y., Meyers, E. M., Bichot, N. P., Serre, T., Poggio, T. A., Desimone, R. (2011). Object decoding with attention in inferior temporal cortex. *Proceedings of the National Academy of Sciences*, 108(21), 8850-8855.
- Zhang, J., Sclaroff, S. (2013). Saliency Detection: A Boolean Map Approach. In *Proceedings IEEE International Conference on Computer Vision*, pp. 153-160.
- Zhang, J., Lin, Z., Brandt, J., Shen, X., Sclaroff, S. (2016). Top-down neural attention by excitation backprop. In *Proceedings of European Conference on Computer Vision*, pp. 543-559.
- Zhaoping Li, (2014). **Understanding vision: theory, models, and data**. Oxford University Press.